

Thermodynamic Analysis of the Heparin Interaction with a Basic Cyclic Peptide Using Isothermal Titration Calorimetry[†]

Ronald E. Hileman,[‡] Robert N. Jennings,[§] and Robert J. Linhardt^{*:‡}

Division of Medicinal and Natural Products Chemistry and Department of Chemical and Biochemical Engineering, University of Iowa, Iowa City, Iowa 52242, and Scios Inc., Mountain View, California 94043

Received January 27, 1998; Revised Manuscript Received July 7, 1998

ABSTRACT: Brain natriuretic peptide (BNP) was examined as part of a continuing study of the interaction of proteins and peptides with the glycosaminoglycan heparin. BNP was tentatively identified as a heparin-binding protein on the basis of its cyclic structure and the high frequency of the basic amino acid residues, lysine and arginine. Thermodynamic analysis using isothermal titration calorimetry confirmed heparin binding to BNP with a micromolar K_d . Surprisingly, despite the high frequency (22%) of basic residues in BNP, only a small portion of the free energy of this interaction resulted from ionic contributions under physiologic conditions. The contribution of polar amino acids, representing 28% of BNP, was next examined in a variety of different buffers. These experiments demonstrated the transfer of five protons from buffer to BNP on heparin binding, suggesting that hydrogen bonding between the polar residues of BNP and heparin is a major factor contributing to the free energy of BNP binding to heparin. Hydrophobic forces apparently play only a small role in binding. Heparin contains few nonpolar functional groups, and a positive change in heat capacity ($\Delta C_p = 1$ kcal/mol) demonstrates the loss of polar residues on BNP–heparin binding.

Previous studies (1, 2) performed in our laboratory have identified structural features within peptides that are important for glycosaminoglycan (GAG)¹ interaction. Specifically, a cyclic peptide structure based on the primary sequence of acidic fibroblast growth factor was found to interact more strongly with the structurally related GAG, heparan sulfate, than a linear peptide having the same sequence. We proposed that the cyclic peptide was structurally similar to the constrained loop structure found in the fibroblast growth factor GAG-binding domain and that the presence of a loop brings the basic amino acids into closer apposition. On the basis of these results, we searched the Swiss PIR, Genbank, and Brookhaven PDB databases for naturally occurring basic cyclic peptides for further studies on the role of loop structures in GAG binding and identified brain natriuretic peptide.

Brain natriuretic peptide, or B-type natriuretic peptide (BNP), is a member of a family of hormones that includes atrial natriuretic peptide (ANP) and C-type natriuretic peptide (CNP). BNP is a 32-amino acid peptide containing a

disulfide bond between C¹⁰ and C²⁶ of the mature peptide forming a 17-residue loop. Natriuretic peptides act as vasodilators and counter the vasoconstriction effects of the renin/angiotensin/aldosterone system (3). BNP is involved in the regulation of salt and water homeostasis (4), blood pressure regulation (5), and vascular remodeling (6). Expression of BNP occurs mainly in the ventricles (6), but it was first isolated from brain (7) as a 134-amino acid precursor that is post-translationally modified to the active form containing 32 residues. BNP is stored in atrial granules (8) and secreted in response to myocardial wall stress (9). BNP's sequence is highly homologous with that of ANP (10), including the disulfide loop structure. In a previous study (11), ANP was shown to interact with heparin, and when ANP was coadministered with heparin, the extents of both the hypotension and diuretic effects of ANP were reduced in rats. Although no reports have characterized BNP as a GAG-binding peptide, its relatively high level of basic residues (approximately 30 mol % and a *pI* of 11) and its loop structure suggested it would interact avidly with the GAG heparin.

Heparin is a repeating copolymer of idouronic (or glucuronic) acid and glucosamine. Due to its high degree of sulfation, heparin is described as a polyelectrolyte. The polyelectrolyte theory, previously developed for thermodynamically characterizing DNA–protein interactions, can also be used for characterizing protein–GAG interactions (12). Polyelectrolytes have a high charge density and, therefore, are associated with multiple counterions in solution. Although the binding of counterions minimizes the repulsive forces within the polyelectrolyte, this binding increases the ordering of the solution and is, thus, entropically disfavored.

[†] This work was supported in part by Scios, Inc., and NIH Grants HL52622 and GM38060 to R.J.L.

^{*} To whom correspondence should be addressed. Fax: (319) 335-6634. E-mail: robert-linhardt@uiowa.edu.

[‡] University of Iowa.

[§] Scios Inc.

¹ Abbreviations: BNP, brain natriuretic peptide; CAPS, 2-(*N*-cyclohexylamino)-1-propanesulfonic acid; CHES, 2-(*N*-cyclohexylamino)ethanesulfonic acid; GAG, glycosaminoglycan; HEPES, *N*-(2-hydroxyethyl)piperazine-*N'*-2-ethanesulfonic acid; GlcNp, glucosamine; IdoAp, iduronic acid; Δ UAp, 4-deoxy- α -L-*threo*-hexenopyranosyluronic acid; S, sulfate; ITC, isothermal titration calorimetry; MES, 2-(*N*-morpholino)ethanesulfonic acid; S, sulfate; Tris, tris(hydroxymethyl)aminomethane; Tricine, *N*-[tris(hydroxymethyl)methyl]glycine.

Upon binding of a protein, these counterions must be displaced from the polyelectrolyte and thus affect the thermodynamics of the interaction. Heparin can also be described as a poly-ol as it contains a large number of hydroxyl groups that can be involved in hydrogen bonding.

This report characterizes the thermodynamics of the brain natriuretic protein (BNP) interaction with heparin using isothermal titration calorimetry (ITC). ITC directly measures the heat released (or absorbed) on ligand binding to a macromolecule. Binding curves are generated by performing multiple injections of the ligand into a solution of the macromolecule. One experiment affords the independent variables ΔH , K_a , and the number of binding sites, n , as well as the dependent variables ΔS and ΔG .

MATERIALS AND METHODS

General. All data were collected using a model 4209 Hart Scientific microtitration calorimeter (Pleasant Grove, UT). The voltage to the instrument was regulated with a Citadel power conditioner (model LC630) from Best Power Technology, Inc. (Necedah, WI), to minimize noise due to voltage fluctuations. A digitally controlled external water bath (model 9109, Polyscience, Niles, IL) was typically set 4–6 °C below the operating temperature for data collection. Chemical calibration was carried out by comparing the observed enthalpy of ionization for Tris to the theoretical value using 10–5 μL injections of 1 mM HCl into 1 mL of 250 mM Tris base at 200 s intervals. Molecular modeling of BNP over the α -carbon backbone of ANP was performed using SYBYL (version 6.1) molecular analysis software from Tripos, Inc. (St. Louis, MO), on a Silicon Graphics workstation.

Preparation of BNP. Recombinant human BNP was cloned as a fusion protein in *Escherichia coli* K12. The BNP peptide was separated from the fusion partner by acid cleavage. The formation of the disulfide bond was accomplished by air oxidation. The peptide was then purified by a series of reversed phase and ion exchange chromatography steps. The purity was >96% on the basis of the percent chromatographic area.

Preparation of Heparin Oligosaccharides. Heparin lyase I was from Sigma Chemical Co. (St. Louis, MO). The enzymatic preparation and structural characterization of the sodium salt of each heparin oligosaccharide, $\Delta\text{UAp}2\text{S}(1\rightarrow4)\text{-}\alpha\text{-D-GlcNpS}6\text{S}$, $\Delta\text{UAp}2\text{S}(1\rightarrow4)\text{-}\alpha\text{-D-GlcNpS}6\text{S}(1\rightarrow4)\text{-}\alpha\text{-L-IdoAp}2\text{S}(1\rightarrow4)\text{-}\alpha\text{-D-GlcNpS}6\text{S}$, $\Delta\text{UAp}2\text{S}(1\rightarrow4)\text{-}\alpha\text{-D-GlcNpS}6\text{S}(1\rightarrow4)\text{-}\alpha\text{-L-IdoAp}2\text{S}(1\rightarrow4)\text{-}\alpha\text{-D-GlcNpS}6\text{S}(1\rightarrow4)\text{-}\alpha\text{-L-IdoAp}2\text{S}(1\rightarrow4)\text{-}\alpha\text{-D-GlcNpS}6\text{S}$, $\Delta\text{UAp}2\text{S}(1\rightarrow4)\text{-}\alpha\text{-D-GlcNpS}6\text{S}(1\rightarrow4)\text{-}\alpha\text{-L-IdoAp}2\text{S}(1\rightarrow4)\text{-}\alpha\text{-D-GlcNpS}6\text{S}(1\rightarrow4)\text{-}\alpha\text{-L-IdoAp}2\text{S}(1\rightarrow4)\text{-}\alpha\text{-D-GlcNpS}6\text{S}(1\rightarrow4)\text{-}\alpha\text{-L-IdoAp}2\text{S}(1\rightarrow4)\text{-}\alpha\text{-D-GlcNpS}6\text{S}$, and $\Delta\text{UAp}2\text{S}(1\rightarrow4)\text{-}\alpha\text{-D-GlcNpS}6\text{S}(1\rightarrow4)\text{-}\alpha\text{-L-IdoAp}2\text{S}(1\rightarrow4)\text{-}\alpha\text{-D-GlcNpS}6\text{S}(1\rightarrow4)\text{-}\alpha\text{-L-IdoAp}2\text{S}(1\rightarrow4)\text{-}\alpha\text{-D-GlcNpS}6\text{S}(1\rightarrow4)\text{-}\alpha\text{-L-IdoAp}2\text{S}(1\rightarrow4)\text{-}\alpha\text{-D-GlcNpS}6\text{S}$ (where ΔUAp is 4-deoxy- α -L-threo-hexenopyranosyluronic acid, GlcNp is 2-amino-2-deoxyglucopyranose, IdoAp is idopyranosyluronic acid, and S is sulfate), having degrees of polymerization of 2, 4, 6, 8, and 10, respectively, have been reported previously (13).

Preparation of Solutions. Stock solutions of both BNP and porcine intestinal mucosal heparin (sodium salt, 167

units/mg, Celsus Laboratories, Cincinnati, OH) were made in distilled deionized water, and the concentration was derived on the basis of reported molecular weights of each [$M_r(\text{BNP}) = 3463$ (0.801 mg of BNP/mg of solid), $M_w(\text{heparin}) = 12\,000$, and $M_w/M_n = 1.3$ (14)]. The commercial heparin used in this study is polydisperse, with molecular weights ranging from 4000 to 25 000. Therefore, all reported thermodynamic values represent averages of the mixture used. A single lot of heparin was used to minimize variation between experiments. BNP and heparin solutions were stored at 4 °C until they were used. Stock solutions of NaCl (2 M), sodium phosphate, Tris-HCl, Tricine/NaOH, and HEPES/NaOH (pH 7.4) (500 mM) were prepared for the buffer-dependent experiments. MES/NaOH (pH 6.0), Tricine/NaOH (pH 8.0), CHES/NaOH (pH 9.1), and CAPS/NaOH (pH 10.5) were prepared at 200 mM for the pH-dependent experiments. Solutions were mixed to obtain the required final concentrations of each component for individual experiments.

Isothermal Titration Calorimetry (ITC) of BNP with Heparin. Titrations of heparin (twenty 5 μL aliquots, 0.45 mM, at either 200 or 300 s intervals) into a solution of BNP (1 mL, 120 μM) were performed in 50 mM buffer containing varying NaCl concentrations. For each NaCl concentration, at least three separate determinations were made. A detailed description of the mathematical model has been previously reported (15–17). For the interaction $M + X \leftrightarrow MX$, the measured parameter between the macromolecule (M) and ligand (X) is the difference in the heat of interaction (ΔQ_i) between the i and $i - 1$ injection. The heat of interaction is expressed as $\Delta Q_i = Q_i - Q_{i-1} = \Delta H[\text{MX}_i - \text{MX}_{i-1}]$, where ΔH is the enthalpy of binding per mole of ligand. The extent of MX complex at injection i is related to the known total ligand concentration $[\text{X}_T]_i$, total macromolecule concentration $[\text{M}_T]_i$, and association constant K . Both $[\text{M}_T]_i$ and $[\text{X}_T]_i$ must be adjusted for dilution at each i th injection volume of X. Thus, $[\text{M}_T]_i = [\text{M}_T]_0 D^i$ and $[\text{X}_T]_i = n[\text{X}_T]_0(1 - D^i)$, where $[\text{M}_T]_0$ and $[\text{X}_T]_0$ represent the initial macromolecule and ligand concentrations, respectively, and D represents the dilution at injection i . Since the concentration of complex is related as $[\text{MX}]_i = [\text{X}_T]_i - [\text{X}]_i$, the positive real root is solved from the following expression, $K[\text{X}]_i^2 + (1 + K[\text{M}_T]_i - K[\text{X}_T]_i)[\text{X}]_i - [\text{X}_T]_i = 0$.

Isothermal Titration Calorimetry (ITC) of BNP with Heparin Oligosaccharides. Titrations of oligosaccharide (twenty 5 μL aliquots, at 300 s intervals) into a solution of BNP (1 mL, 120 μM) were performed in 50 mM sodium phosphate buffer (pH 7.4). The concentration used for each oligosaccharide having a degree of polymerization of 2, 4, 6, 8, and 10 was 9, 6, 3, 3, and 1.15 mM, respectively. Concentrations were calculated by UV spectroscopy in 30 mM HCl using an $\epsilon_{232\text{nm}}$ of $5200\text{ M}^{-1}\text{ cm}^{-1}$ (18).

RESULTS

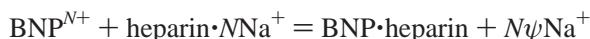
The sequence and amino acid composition of mature BNP is shown in Table 1. Inspection of the sequence reveals that BNP contains a number of residues that could potentially interact with heparin. The α -carbon backbone of ANP has been determined by NMR (19), and molecular modeling of the BNP sequence over the ANP structure (not shown) suggests that the loop structure produced by the disulfide

Table 1: Sequence and Amino Acid Composition Analysis of BNP

Composition	
amino acids	% by frequency
basic (KR)	22
polar (NCQSTY)	28
acidic (DE)	3
hydrophobic (AILFWV)	19

bond brings several basic and polar residues into close apposition. We investigated the possibility that BNP is a heparin-binding protein using isothermal titration calorimetry. A representative titration is shown in Figure 1. The peaks (panel A) correspond to an exothermic interaction. The peak area diminished with each new injection of heparin. The small peaks of constant area seen near the end of the titration (injections 15–20) correspond to the heat of dilution for heparin. In a separate experiment, the heat of dilution for heparin was determined by injecting heparin into buffer in the absence of BNP. This constant was subtracted from the raw data (panel A) to obtain the microjoules of heat evolved from each injection (panel B). The similarity between the fitted curve and the integrated peak areas (panel B) is consistent with the noncompetitive multisite interaction model (see Materials and Methods) used to describe this interaction.

Effect of Salt on the BNP–Heparin Interaction. A polyelectrolyte, such as heparin, is associated with bound counterions (e.g., Na^+). These counterions are released when heparin binds to its ligand, BNP. The equilibrium is described as follows (20).



N represents the number of counterions released, and the term ψ describes the fraction of counterion bound per unit charge. The term ψ depends on the axial charge density of the polyelectrolyte and has been both mathematically and experimentally determined for heparin to be 0.8 (21, 22). Due to the entropically unfavorable ordering of Na^+ on the heparin polyanion, a fraction of the free energy of protein binding is derived from the release of Na^+ . The overall interaction of protein with heparin is comprised of both an ionic and nonionic component. The ionic component, described by the favorable release of Na^+ from heparin by a cation within the protein (such as an arginine or lysine residue), is termed the polyelectrolyte effect (20, 23). The nonionic component may involve interactions such as hydrogen bonding or hydrophobic interaction. The overall interaction can be described as follows.

$$\log K_d = \log K_{d(\text{nonionic})} + N\psi \log[\text{Na}^+]$$

This equation suggests that the extent of protein binding to heparin will decrease with increasing NaCl concentrations, as is commonly observed for heparin-binding proteins. A plot of $\log[\text{NaCl}]$ versus $\log K_d$ yields a line with a y-intercept and slope corresponding to the nonionic contribution and number of ions released multiplied by ψ (Figure 2), respectively. The percent nonionic contribution to the total energy of binding is dependent on the NaCl concentration. At physiologic ionic strength [50 mM sodium phos-

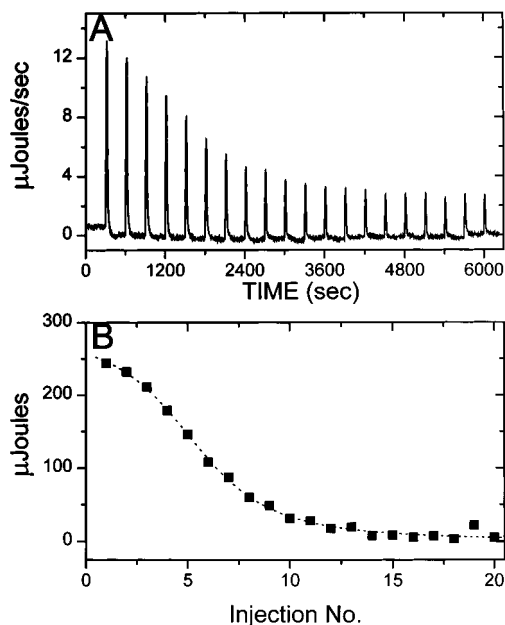


FIGURE 1: Representative titration of BNP with heparin in 50 mM phosphate buffer (pH 7.4) containing 50 mM NaCl at 25 °C. (A) Raw data. BNP (1 mL, 120 μM) was titrated with heparin (100 μL , 450 μM). Each injection volume was 5 μL . (B) Integrated data. Peak areas in panel A were fitted using an iterative nonlinear least-squares algorithm that varies ΔH , K_a , and n . The fitted data (dotted line) describes an interaction with a ΔH of -28.7 kcal/mol, a K_d of 1.78 μM , and a stoichiometry (n) of 9.92 mol of BNP per mole of heparin.

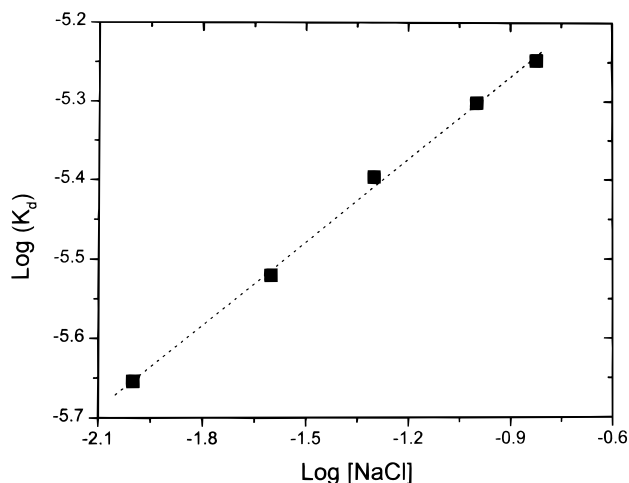


FIGURE 2: Effect of salt on the BNP–heparin interaction. Linear regression analysis was used to obtain the dotted line which corresponds to a y-intercept of -5 and a slope of 0.4. At the y-intercept, $[\text{Na}^+]$ is 1 M and corresponds to a K_d of 11 μM and a ΔG of -6.8 kcal/mol.

phate and 150 mM NaCl (pH 7.4)], the K_d was determined to be 5.6 μM (Table 2). Extrapolation of the data to 1 M Na^+ affords the nonionic contribution (the y-intercept was -5 , or a K_d of 11 μM ; see the legend of Figure 2). Comparison of the binding free energy at a selected ionic strength with the nonionic binding free energy can be used to describe the percent ionic contribution and is only 6% [at 25 °C, with 150 mM NaCl, in 50 mM sodium phosphate buffer (pH 7.4)]. When the value for ψ (0.8) is taken into account, the slope of the plot (Figure 2) yields the number of Na^+ ions displaced per BNP interaction and corresponds to 0.5 Na^+ ion.

Table 2: Effect of Salt on the Thermodynamic Values for the Interaction of BNP with Heparin^a

[NaCl] (M)	total [Na ⁺] (M)	K_d (μ M)	ΔG_{obs} (kcal/mol)	n (no. of BNPs per heparin chain)	ΔH_{obs} (kcal/mol)
0.010	0.1005	2.2 ± 1.3	-7.82 ± 0.31	12.3 ± 1.3	-39.4 ± 7.3
0.025	0.1155	3.0 ± 0.8	-7.66 ± 0.13	13.6 ± 2.4	-36.9 ± 3.1
0.050	0.1405	4.0 ± 0.3	-7.36 ± 0.04	10.4 ± 0.8	-27.9 ± 4.4
0.100	0.1905	5.0 ± 0.4	-7.23 ± 0.05	7.6 ± 1.4	-6.8 ± 1.0
0.150	0.2405	5.6 ± 0.1	-7.16 ± 0.01	6.6 ± 0.1	-2.3 ± 0.6

^a All data were collected in 50 mM sodium phosphate buffer (pH 7.4) containing the indicated amount of NaCl, at 25 °C. The total [Na⁺] was calculated as the sum of sodium ion concentrations from 50 mM sodium phosphate buffer (0.0905 M) and the added NaCl. Each salt concentration is reported as an average and average deviation of at three separate determinations.

While the change in K_d as a function of salt concentration is well behaved, Table 2 also shows an unexpected and significant (2-fold) change in the stoichiometry of interaction, n . Furthermore, the ΔH_{obs} shows an even greater change (17-fold) over the same range of salt concentrations, including an abrupt change, ΔH_{obs} going from -27.9 to -6.8 kcal/mol, between 0.05 and 0.10 M NaCl. These changes in both n and ΔH_{obs} suggest a change in the mode of binding is taking place as the salt concentration becomes high. Thus, caution must be used in interpreting Figure 2. While the precise number of sodium ions released may not be definitively established from Figure 2, it remains clear that a small number of Na⁺ ions are displaced on BNP binding.

On the basis of a weight-averaged molecular weight of 12 000 for heparin and a sequence corresponding to the repeating disaccharide unit $\rightarrow 4$ - α -L-IdoAp2S(1 \rightarrow 4)- β -D-GlcNpS6S(1 \rightarrow with a molecular weight of 665, the number of disaccharides per heparin chain is 18 (12000/665). With 150 mM NaCl and 50 mM sodium phosphate, we observed 6.6 BNP molecules binding per heparin chain (Table 2). Thus, these data show that under physiologic conditions a hexasaccharide is the smallest interacting species (three disaccharides \approx 18/6.6).

Effect of the Degree of Polymerization on the BNP–Heparin Interaction. Although the observed K_d for the BNP–heparin interaction increased with increasing NaCl concentration as expected, the stoichiometry of interaction varied (Table 2). This result is not predicted by the polyelectrolyte theory. In addition, the inherent polydispersity [$M_w/M_n \sim 1.3$ (14)] of heparin might further complicate the calculation of the minimum number of BNP binding sites in heparin. To definitively establish the number of sugar residues that interact with BNP, structurally defined, monodisperse oligosaccharides were prepared by partial heparin lyase I treatment of heparin (13). The structure of the oligosaccharides used was Δ UAp2S(1 \rightarrow 4)- α -D-GlcNpS6S-(1 \rightarrow 4)- α -L-IdoAp2S(1 \rightarrow) _{n} GlcNpS6S, where $n = 0, 2, 4, 6,$ and 8 for disaccharide through deca-saccharide, respectively. Table 3 shows the effect of heparin oligosaccharide chain length on the interaction of BNP. Consistent with the stoichiometry of BNP–heparin binding, a heparin hexasaccharide, Δ UAp2S(1 \rightarrow 4)- α -D-GlcNpS6S(1 \rightarrow 4)- α -L-IdoAp2S(1 \rightarrow 4)- α -D-GlcNpS6S(1 \rightarrow 4)- α -L-IdoAp2S(1 \rightarrow 4)- α -D-GlcNpS6S, was the smallest interacting species with an observed 1:1 molar ratio (K_d of 34 μ M). The heparin

Table 3: Effect of the Degree of Polymerization on the Thermodynamic Values for the Interaction of BNP with Monodisperse Heparin Oligosaccharides^a

degree of polymerization	K_d (μ M)	n (no. of BNP per oligosaccharide)	ΔH_{obs} (kcal/mol)
2	> 1000	nd ^b	nd
4	240	0.5	-1.7
6	34	1.1	-6.5
8	20	1.0	-7.6
10	12	0.9	-12.2

^a All data were collected in 50 mM sodium phosphate buffer (pH 7.4) at 25 °C. ^b Not determined due to insufficient heat of interaction.

Table 4: Effect of Buffer on the Thermodynamic Values for the Interaction of BNP with Heparin^a

buffer	ΔH_{ion} (kcal/mol)	n (no. of BNP per heparin)	ΔG (kcal/mol)	ΔH_{obs} (kcal/mol)
HEPES	3.9	8.7 ± 0.1	-9.65 ± 0.03	-55.4 ± 1.2
MOPS	5.29	9.4 ± 0.1	-9.36 ± 0.06	-50.7 ± 1.5
Tricine	7.76	9.2 ± 0.1	-8.83 ± 0.03	-36.1 ± 0.1
Tris	11.51	10.1 ± 0.1	-8.02 ± 0.3	-15.2 ± 2.3

^a All data were collected in the indicated buffer (50 mM, pH 7.4) containing 25 mM NaCl, at 25 °C in triplicate.

tetrasaccharide interaction with BNP was considerably weaker (K_d of 240 μ M) with an observed ratio of two tetrasaccharides per BNP. Oligosaccharides with a degree of polymerization of 8 and 10 bound BNP with greater affinity than the hexasaccharide and had increased heats of binding but were not sufficiently large to accommodate two BNP molecules. Due to the relatively large amounts of oligosaccharide required (~ 7 mg per titration) and the difficulties in their preparation and purification, these experiments were not repeated at varying NaCl concentrations.

Effect of Buffer on the BNP–Heparin Interaction. Although the observed enthalpy of interaction (ΔH_{obs}), obtained from an ITC experiment, is normally used to describe the binding event, solvent contributions may also be involved. For example, proton(s) from the buffer may be consumed during the interaction. The relatively small ionic contribution to the observed free energy for the interaction of BNP with heparin suggests that this interaction is almost entirely due to hydrogen bonding. Hydrophobic interactions are not generally important for interactions with heparin since the only hydrophobic group in its structure is an acetamide functionality of GlcNpAc (where Ac is acetate), which occurs approximately once per heparin chain (24). The number of protons involved in the interaction of BNP with heparin was determined by performing titrations in several buffers having known enthalpies of ionization (21, 25) (Table 4). The observed enthalpy of interaction (ΔH_{obs}) is linearly related to the enthalpy of buffer ionization (ΔH_{ion}) as follows (26).

$$\Delta H_{\text{obs}}^{\circ} = \Delta H_{\text{int}}^{\circ} + N\Delta H_{\text{ion}}^{\circ}$$

The y-intercept, ΔH_{int} , is the intrinsic enthalpy of the interaction, and the slope, N , is the number of protons either abstracted from the buffer (positive value) or donated to the buffer (negative value). A plot of ΔH_{ion} versus ΔH_{obs} (Figure 3) shows that approximately five protons are abstracted from the buffer per BNP molecule. The y-intercept gave an intrinsic enthalpy, ΔH_{int} , of -77.8 kcal/mol. As reported

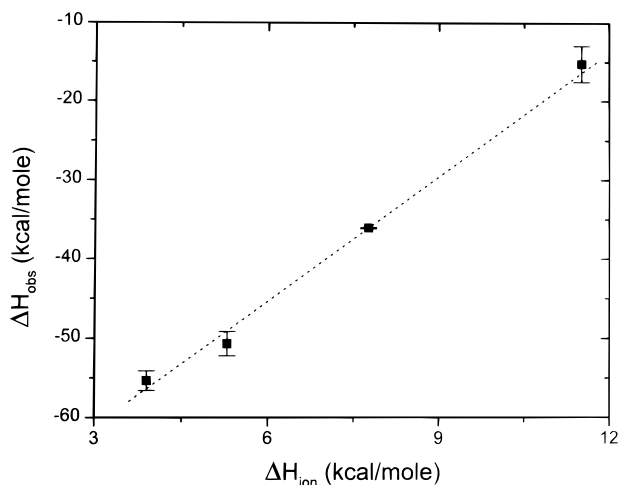


FIGURE 3: Effect of temperature on the BNP–heparin interaction. Linear regression analysis (dotted line) yields a slope (ΔC_p) of 1 kcal/mol and a y-intercept of -361 kcal/mol.

Table 5: Effect of pH on the Thermodynamic Values for the Interaction of BNP with Heparin^a

buffer	pH	pK _a	<i>n</i> (no. of BNPs per heparin)	K _d (μM)	ΔH _{obs} (kcal/mol)
MES	6.0	6.1	9.52	0.19	−34.1
Tricine	7.4	8.1	9.2	0.14	−50.7
Tricine	8.0	8.1	11.4	0.74	−39.9
CHES	9.2	9.3	10.1	0.99	−40.3
CAPS	10.5	10.4	10.5	4.25	−62.8

^a All data were collected in the indicated buffer (50 mM, at the indicated pH) containing 25 mM NaCl, at 25 °C.

previously in Table 2, a change in *n* was also observed with buffer (Table 4). This change was neither large nor consistent. The *n* value is the least reliable term in any fit because a small error in the concentration of both BNP and heparin can lead to a large error in *n*. While replicate analysis was performed (Table 4), these were not independent replicates, as the same stock solutions of BNP and heparin were used to perform ITC in triplicate. Thus, the modest variation in *n* with different buffers can most likely be ascribed to errors in concentrations.

Effect of pH on the BNP–Heparin Interaction. The pH dependency of the BNP–heparin interaction was next investigated (Table 5). Each titration was performed near the pK_a of the buffer to ensure good buffering capacity. Separate studies of the effect of each buffer on the interaction were not undertaken. However, the small variation in *n* suggests that pH does not influence the stoichiometry of this interaction. The K_d was observed to increase with increasing pH. While it is possible to rule out changes in the protonations of certain functional groups in the range of pH 6.0–10.5 [i.e., the *N*-sulfo and *O*-sulfo groups of heparin have pK_a values of 0.5–1.5 (27)], others such as carboxylate groups may play a role. The average heparin chain contains 18 carboxylate groups, and BNP has two, the C terminus and D. The pK_a values of the carboxylate groups in heparin are reported as 3.1; however, because heparin is a polyelectrolyte, their pK_a is concentration-dependent and may be substantially higher. In addition, a carboxy group in a hydrophobic domain of an interacting complex might show a pK_a in the neutral pH range.

Table 6: Temperature-Dependent Thermodynamic Values for the Interaction of BNP with Heparin^a

<i>T</i> (°C)	<i>n</i> (no. of BNPs per heparin)	Δ <i>H</i> (kcal/mol)	Δ <i>G</i> (kcal/mol)	<i>T</i> Δ <i>S</i> (kcal/mol)
15	12.1	−57.6	−7.4	−50.3
20	11.2	−47.0	−7.7	−39.4
25	15.3	−38.5	−7.6	−30.9
30	11.5	−49.9	−8.1	−41.8
35	11.2	−36.2	−7.9	−28.3
40	9.6	−26.3	−8.3	−18.0
45	10.0	−22.7	−8.0	−14.7

^a All data were collected in 50 mM sodium phosphate buffer (pH 7.4) containing 25 mM NaCl, at the indicated temperature, and are reported as the average of duplicate determinations.

Effect of Temperature on the BNP–Heparin Interaction. The effect of temperature was investigated in sodium phosphate buffer (Table 6). The slope of the relationship of Δ*H*_{obs} versus *T* (not shown) describes the heat capacity change, Δ*C*_{*p*}, for the BNP–heparin interaction. The large positive value for Δ*C*_{*p*} of 1 kcal/mol indicates a loss of polar residues on the surface of BNP. This is expected for interactions of protein with a highly charged molecule such as heparin. Extrapolation to 0 K yields a y-intercept of -361 kcal/mol.

DISCUSSION

Previous studies from our laboratory, in which a variety of physical and chemical methods were used on a variety of heparin-binding peptides, suggested the importance of multiple arginine and lysine residues conformationally constrained in a closed loop (1, 2). Modeling studies on known heparin-binding proteins also suggested the importance of secondary structure in the topology of GAG binding sites (1, 2). A search for conformationally constrained peptides rich in basic amino acid residues suggested that we examine the cyclic peptide BNP as a possible GAG-binding peptide. A detailed search of the literature revealed no information suggesting that BNP was a heparin-binding peptide. Interestingly, a chondroitin sulfate proteoglycan, having a GAG chain structurally related to heparin, has been shown to be secreted from cardiomyocytes under the same conditions that induce BNP (28). Perhaps this natriuretic peptide is stored on the GAG chains of this proteoglycan and is released in response to neuroendocrine stimuli as a peptide–GAG complex.

Initial examination by isothermal titration calorimetry confirmed that BNP interacted with heparin with a micromolar K_d consistent with our expectations. BNP contains seven possible charged basic residues (excluding histidine which is uncharged at pH 7.4) corresponding to 22% of its structure. This high content of basic residues suggested that the interaction between BNP and heparin was primarily the result of ionic interaction. Record analysis (20) was used in an attempt to confirm this assumption.

The negatively charged sulfate (and carboxylate) groups present in heparin are typically ion-paired with positively charged sodium ions. Due to the entropically unfavorable ordering of Na⁺ on the heparin polyanion, a fraction of the free energy of protein binding is derived from the release of Na⁺. The overall interaction of protein with heparin is comprised of both an ionic and nonionic component. The

ionic component, described by the favorable release of Na^+ from heparin by a cationic residue within the protein (such as the guanidinium group of arginine or the ammonium group of lysine), is termed the polyelectrolyte effect. The nonionic component may involve interactions such as hydrogen bonding or hydrophobic interaction. By experimentally determining the overall K_d at multiple Na^+ concentrations, we can calculate the contribution of the polyelectrolyte effect.

Using polyelectrolyte theory, the degree of ionic character for the interaction of BNP with heparin was determined. Surprisingly, the observed value was $\sim 6\%$ ionic component for BNP–heparin binding. While the unexpected increase in n with ionic strength complicates the interpretation of the precise level of the ionic contribution to heparin–BNP interaction, it is certainly much lower than that reported for other heparin-binding proteins. For example, basic fibroblast growth factor (bFGF) (21), antithrombin III (ATIII) (29), thrombin (22), and secretory leukocyte proteinase inhibitor (SLPI) (30, 31) display 30, 40, 80, and 85% ionic contributions, respectively.

The consistent decrease in n with increased ionic strength when coupled with the dramatic change in ΔH_{obs} between 0.05 and 0.1 M NaCl suggests the mode of BNP–heparin binding is being altered at higher salt concentrations. At low salt concentrations, the interaction between the acidic heparin polyanion and the basic BNP peptide relies on both a hydrogen-bonding and an ionic component. At higher ionic strengths (i.e., 0.1 M added NaCl), the interactions between the positively charged residues (i.e., R and K) of BNP and the heparin polyanion are broken. These positively charged residues are exposed, causing the repulsion of the neighboring heparin-bound BNP molecules. This results in a decreased n and a less negative ΔH_{obs} . In essence, at high salt concentrations, a negative cooperativity is observed.

ITC of BNP with monodisperse heparin oligosaccharides clearly shows that a hexasaccharide is the smallest interacting species. The hexasaccharide affinity (K_d of 34 μM) was lower than that observed for heparin (K_d of 2.2 μM) under similar conditions. This suggests that other sequences present in heparin may contribute to the interaction or that the unusual ΔUAp residue [a product of the heparin lyase eliminase reaction (24)] may interfere with BNP interaction.

The major ($\sim 94\%$) contribution to the free energy of BNP binding to heparin could come from either hydrophobic or hydrogen bonding interactions. ITC analysis of the BNP–heparin interaction in various buffers clearly demonstrated that five protons were abstracted from the buffer for each molecule of BNP binding to heparin. These results suggest that hydrogen bonding between BNP and heparin is responsible for most of the free energy of binding. The five protons abstracted from the buffer might be transferred to carboxylate groups within heparin or BNP, although this remains to be demonstrated. Seven polar residues (excluding the two cystines forming a disulfide linkage) are also likely participants in hydrogen bonding interaction with the hydroxyl or carboxyl groups of heparin. Of particular note is the cluster of four serine residues in the loop structure of BNP.

While hydrophobic interaction between the highly polar BNP and heparin is unlikely, we decided to measure the change in heat capacity in binding to confirm that nonpolar interactions were not a major contributor to the free energy of binding. The temperature dependence of the ΔH_{obs} for

the BNP–heparin interaction was determined to be 1 kcal/mol. For protein–protein interactions, negative ΔC_p values are normally observed, corresponding to a reduction in the number of nonpolar surface-exposed residues. For the BNP–heparin interaction, we expected that the predominant driving forces are ionic and polar in nature. The positive ΔC_p confirmed a reduction in the number of polar surface-exposed residues. The heat capacity of binding has been shown to be extremely useful in predicting the surface-exposed polar and nonpolar surface area change upon ligand binding (26, 32). Since no structural data are available for BNP, calculations quantifying the change in water-accessible nonpolar surface area cannot be performed.

In conclusion, while the presence of a loop structure rich in basic amino acid residues suggested that BNP was a heparin-binding protein, the molecular basis for this interaction had little to do with the abundance of these amino acid residues. This study points out the importance of the often overlooked polar amino acid residues in promoting protein–GAG interaction through hydrogen bonding. This study also demonstrates the value of ITC in performing detailed analysis of such interactions.

ACKNOWLEDGMENT

We thank Professor Kenneth P. Murphy of the University of Iowa for helpful discussions on the interpretation of results presented in this paper.

REFERENCES

- Fromm, J. R., Hileman, R. E., Caldwell, E. E. O., Weiler, J. M., and Linhardt, R. J. (1997) *Arch. Biochem. Biophys.* **343**, 92–100.
- Fromm, J. R., Hileman, R. E., Weiler, J. M., and Linhardt, R. J. (1997) *Arch. Biochem. Biophys.* **346**, 252–262.
- Nicholls, D. P., Onuoha, G. N., McDowell, G., Elborn, J. S., Riley, M. S., Nugent, A. M., Steele, I. C., Shaw, C., and Buchanan, K. D. (1996) *Basic Res. Cardiol.* **91**, 13–20.
- Meyer, M., Stief, C. G., Becker, A. J., Truss, M. C., Taher, A., Jonas, U., and Forssmann, W. G. (1996) *World J. Urol.* **14**, 375–379.
- Ogawa, Y., Itoh, H., and Nakao, K. (1995) *Clin. Exp. Pharmacol. Physiol.* **22**, 49–53.
- Zhang, L., Xu, D., West, M. J., and Summers, K. M. (1997) *Clin. Exp. Pharmacol. Physiol.* **24**, 442–444.
- Sudoh, T., Kangawa, K., Minamino, N., and Matsuo, H. (1988) *Nature* **332**, 78–81.
- Thibault, G., Charbonneau, C., Bilodeau, J., Schiffrin, E. L., and Garcia, R. (1992) *Am. J. Physiol.* **263**, R301–R309.
- Klinge, R., Djøseland, O., Karlberg, B. E., and Hall, C. (1997) *Clin. Pharmacol.* **17**, 389–400.
- Hino, J., Tateyama, H., Minamino, N., Kangawa, K., and Matsuo, H. (1990) *Biochem. Biophys. Res. Commun.* **167**, 693–700.
- Wei, Y., Holmberg, S. W., Leahy, K. M., Olins, P. O., Devine, C. S., and Needleman, P. (1987) *Hypertension* **9**, 607–610.
- Hileman, R. E., Fromm, J. R., Weiler, J. M., and Linhardt, R. J. (1998) *BioEssays* **20**, 156–167.
- Pervin, A., Gallo, C., Jandik, K., Han, X.-J., and Linhardt, R. J. (1995) *Glycobiology* **5**, 83–95.
- Edens, R. E., Al-Hakim, A., Weiler, J. M., Rethwisch, D. G., Fareed, J., and Linhardt, R. J. (1992) *J. Pharm. Sci.* **81**, 823–827.
- Freire, E., Mayorga, O. L., and Straume, M. (1990) *Anal. Chem.* **62**, 950A–959A.
- Wiseman, T., Williston, S., Brandts, J. F., and Lin, L.-N. (1989) *Anal. Biochem.* **179**, 131–137.
- Connelly, P. R., Varadarajan, R., Sturtevant, J. M., and Richards, F. M. (1990) *Biochemistry* **29**, 6108–6114.

18. Rice, K. G., and Linhardt, R. J. (1989) *Carbohydr. Res.* 190, 219–233.
19. Fairbrother, W. J., McDowell, R. S., and Cunningham, B. C. (1994) *Biochemistry* 33, 8897–8904.
20. Record, T. M., Lohman, T. M., and de Haseth, P. J. (1976) *J. Mol. Biol.* 107, 145–158.
21. Thompson, L. D., Pantoliano, M. W., and Springer, B. A. (1994) *Biochemistry* 33, 3831–3840.
22. Olson, S. T., Halvorson, H. R., and Bjork, I. (1991) *J. Biol. Chem.* 266, 6342–6352.
23. Lohman, T. M., and Mascotti, D. P. (1992) *Methods Enzymol.* 212, 400–424.
24. Linhardt, R. J., Toida, T., Smith, A. E., and Hileman, R. E. (1997) in *A Laboratory Guide to Glycoconjugate Analysis* (Gallagher, J. T., and Jackson, P., Eds.) pp 183–197, Birhauser Verlag AG, Basel, Switzerland.
25. Morin, P. E., and Freire, E. (1991) *Biochemistry* 30, 8494–8500.
26. Baker, B. M., and Murphy, K. P. (1997) *J. Mol. Biol.* 268, 557–569.
27. Wang, H. L., Loganathan, D., and Linhardt, R. J. (1991) *Biochem. J.* 278, 689–695.
28. Gorr, S.-U., and Pence, S. S. (1995) *J. Mol. Cell Cardiol.* 27, 767–771.
29. Olson, S. T., and Bjork, I. (1991) *J. Biol. Chem.* 266, 6353–6364.
30. Faller, B., Mely, Y., Gerard, D., and Bieth, J. G. (1992) *Biochemistry* 31, 8285–8290.
31. Fath, M. A., Wu, X., Hileman, R. E., Linhardt, R. J., Abraham, W. M., Kashem, M. A., Nelson, R. M., and Wright, C. (1998) *J. Biol. Chem.* 273, 13563–13569.
32. Spolar, R. S., Ha, J.-H., and Record, M. T. (1989) *Proc. Natl. Acad. Sci. U.S.A.* 86, 8382–8385.

BI980212X